

**PREDICTING RESIDUAL STIFFNESS OF CRACKED COMPOSITE
LAMINATES SUBJECTED TO MULTI-AXIAL INPLANE LOADING**

M. Kashtalyan* and C. Soutis**

*Centre for Micro- and Nanomechanics (CEMINACS), School of Engineering,
University of Aberdeen, Aberdeen, AB24 3UE, UK

m.kashtalyan@abdn.ac.uk

** School of Mechanical, Aerospace & Civil Engineering, University of Manchester,
Manchester M13 9PL

constantinos.soutis@manchester.ac.uk

Abstract

This is a contribution to the exercise that aims to benchmark and validate the current continuum damage and fracture mechanics methodologies used for predicting the mechanical behaviour of fibre reinforced plastic composites under complex loadings. The paper describes an analytical approach to predict the effect of intra- (matrix cracking and splitting) and inter-laminar (delamination) damage on the residual stiffness properties of the laminate which can be used in the post-initial failure analysis, taking full account of damage mode interaction. The approach is based on a two-dimensional shear lag stress analysis and the Equivalent Constraint Model (ECM) of the damaged laminate with multiple damaged plies. The application of the approach to predicting degraded stiffness properties of a multidirectional laminate with multilayer inter- and interlaminar damage is demonstrated for $[0/90/0]$ and $[0/90_8/0]$ cross-ply laminates made from a specific glass/epoxy system under in-plane uniaxial and biaxial loading damaged by transverse and longitudinal matrix cracks and crack-induced transverse and longitudinal delamination.

Keywords: A. Polymer-matrix composites (PMCs); B. Matrix cracking; C. Damage mechanics; C. Transverse cracking

LIST of SYMBOLS

s_1	Half-spacing between longitudinal cracks
s_2	Half-spacing between transverse cracks
ℓ_1	Half-length of longitudinal delamination
ℓ_2	Half-length of transverse delamination
$\bar{\sigma}_{11}, \bar{\sigma}_{22}, \bar{\sigma}_{12}$	In-plane loading
μ ($\mu = 1, 2$)	Index denoting explicitly damage layer
κ ($\kappa = 1, 2; \kappa \neq \mu$)	Index denoting equivalently constraining layer
x_1, x_2, x_3	Cartesian co-ordinates
$\tilde{\sigma}_{pq}^{(\mu, k)}$	In-plane microstresses in the k^{th} layer of the ECM μ laminate (i.e. stresses averaged across the thickness of the k^{th} layer layer and the width of the laminate)
$\tau_1^{(\mu)}, \tau_2^{(\mu)}$	Peak shear stresses at the peak shear stresses at the (0/90) interface of the ECM μ in the $x_\mu 0 x_3$ plane
h_k	Thickness of the k^{th} layer
w_μ	Width of the ECM μ laminate
χ	Layer thickness ratio h_1 / h_2
$[\hat{Q}^{(\mu)}]$	In-plane stiffness matrix of the explicitly damaged layer
$[Q^{(\kappa)}]$	In-plane stiffness matrix of the homogeneous orthotropic material of the equivalently constraining κ^{th} layer
$[\hat{S}^{(\mu)}]$	Compliance matrix of the explicitly damaged layer
$[S^{(\kappa)}]$	Compliance matrix of the homogeneous orthotropic

	material of the equivalently constraining κ^{th} layer
$\tilde{\varepsilon}_1^{(\mu,k)}, \tilde{\varepsilon}_2^{(\mu,k)}, \tilde{\varepsilon}_6^{(\mu,k)}$	In-plane microstrains in the k^{th} layer of the ECM μ laminate (i.e. strains averaged across the thickness of the k^{th} layer layer and the width of the laminate)
$u_1^{(\mu,k)}, u_2^{(\mu,k)}$	In-plane displacements in the k^{th} layer of the ECM μ laminate
h_s	Thickness of the shear layer
m_s	Number of plies in the shear layer
t	Nominal ply thickness
K_1, K_2	Shear lag parameter
$\hat{G}_{13}^{(k)}, \hat{G}_{23}^{(k)}$	Out-of-plane shear moduli of the k^{th} layer
$L_1^{(\mu)}, L_1^{(\mu)}$	Laminate constants
$\Omega_{11}^{(\mu)}, \Omega_{22}^{(\mu)}, \Omega_{12}^{(\mu)}$	Laminate constants
$\bar{\sigma}_{pq}^{(\mu,k)}$	In-plane macrostresses in the k^{th} layer of the ECM μ laminate
$\bar{\varepsilon}_1^{(\mu,k)}, \bar{\varepsilon}_2^{(\mu,k)}, \bar{\varepsilon}_6^{(\mu,k)}$	In-plane macrostrains in the k^{th} layer of the ECM μ laminate
$\Lambda_{22}^{(\mu)}, \Lambda_{66}^{(\mu)}$	In-situ Damage Effective Functions for the ECM μ laminate
$D_\mu^{mc} = h_\mu / s_\mu$	Relative crack density
$D_\mu^{ld} = \ell_\mu / s_\mu$	Relative delamination area
ρ_G, ρ_G^*	Shear modulus reduction ratios

1 INTRODUCTION

Failure process of fibre-reinforced composite laminates subjected to quasi-static, tensile fatigue or thermal loading involves sequential accumulation of intra- and interlaminar damage in the form of matrix cracking and delamination. Intralaminar matrix cracks parallel to the fibres in the off-axis plies is the first damage mode observed. Depending on the laminate stacking sequence, these cracks are either arrested at the interface or cause interfacial failure leading to delamination and/or cracking in the adjacent layers due to high interlaminar stresses at the interface. Development of intra- and interlaminar damage in composite laminates has been the subject of numerous studies in the literature, see e.g. our reviews (Kashtalyan and Soutis, 2002; 2005).

Multidirectional laminates subjected to uniaxial or biaxial stresses may still be capable of carrying load after first ply failure or initial failure has occurred. In the laminate, in-plane shear and normal stresses can be transferred, to some extent, back into the damaged lamina via the neighbouring laminae. Owing to this stress transfer damaged lamina within the laminate retains certain amount of load-carrying capacity. In-situ stiffness of a damaged lamina constrained within the laminate depends on the damage configuration and stiffnesses and thicknesses of neighbouring laminae.

Prediction of the post-initial failure behaviour of a laminate requires accurate information regarding the properties of the damaged lamina.

The post-initial failure models employed in the failure theories can be classified into two main groups: (i) models employing sudden reduction in the properties of the failed lamina; (ii) models employing a gradual drop in the properties of the failed lamina.

The five failure theories by Zinoviev (Zinoviev et al, 1998; 2002), Boggetti (Bogetti et al, 2004a; 2004b), Tsai (Liu and Tsai, 1998; Kuraishi et al, 2002), Puck (Puck and Schürmann, 1998; 2002) and Cuntze (Cuntze and Freund, 2004; Cuntze, 2004) have been identified as the most reliable by the quantitative assessment procedure carried out within the previous WWFE (Kaddour et al, 2004); all five incorporate post-initial failure analysis.

Zinoviev (Zinoviev et al, 1998; 2002) used the maximum stress failure criterion with a carefully developed post-failure analysis. Linear elastic stress-strain behaviour up to initial failure was assumed but a continuous correction for the effects of change of fibre orientation throughout loading was included in the theory. Boggetti (Bogetti et al, 2004a; 2004b) used a three-dimensional form of the Maximum Strain failure criterion with allowance for non-linear lamina shear stress-strain behaviour and a simple progressive failure analysis. Tsai (Liu and Tsai, 1998; Kuraishi et al, 2002) employed the well-known Tsai-Wu interactive failure criterion that does not explicitly identify failure mechanisms, assumed linear elastic material properties and reduced matrix stiffness after initial failure. The theories used by Puck (Puck and Schürmann, 1998; 2002) and Cuntze (Cuntze and Freund, 2004; Cuntze, 2004) considered three-dimensional failure mechanisms in some detail and applied non-linear analysis to predict progressive failure. Cuntze's approach is similar to Puck's in some respects but assumes interaction between failure modes due to probabilistic effects. These two theories produced the highest number of accurate predictions (i.e. within 10% of the measured values) and captured more general features of the experimental results and laminate behaviour in the ranking study than the other theories.

The only theory identified in Soden et al (2004) as performing well in predicting

crack density was McCartney's theoretical approach (McCartney, 1998; 2002), which used detailed mathematical analysis for reducing stiffness properties of the laminates due to matrix cracking in the inner ply of the laminate. In its present form, the theory does not take into account the presence and interaction of other damage modes in the same and/or the adjacent plies of multidirectional laminates. Comparisons of this theory with other approaches are given in Kashtalyan and Soutis (2006) and Zhang et al (2006).

There is a great deal of interest in the validation of failure criteria and this has led to two international exercises being coordinated at the present time. These are the Second World-Wide Failure Exercise (WWFE-II), which deals with benchmarking triaxial (3D) failure criteria and the Third World-Wide Failure Exercise (WWFE-III), which is concerned with benchmarking damage models for fibre reinforced composites, see Kaddour et al (2012b, 2012c, 2012d). The WWFE-II has been completed and its outcome is fully described by Kaddour and Hinton (2012a).

This paper is the authors' contribution to WWFE-III. It describes one of the leading methods of predicting the effect of intra- and inter-laminar damage on the stiffness properties of the laminate which can be used in the post-initial failure analysis, taking full account of damage mode interaction. The approach is based on the Equivalent Constraint Model (ECM) of the damaged laminate. Closed form expressions are given for the In-situ Damage Effective Functions which characterise degraded stiffness properties of each damaged ply; for a given damaged ply they explicitly depend on the damage parameters (matrix crack density and relative delamination area) associated with that ply and implicitly on the damage parameters associated with other damaged plies.

The application of the approach to predict the degraded stiffness properties of multidirectional laminate with multilayer inter- and interlaminar damage is shown for for $[0/90/0]$ and $[0/90_8/0]$ cross-ply laminates made from a glass fibre/LY556 epoxy material system under uniaxial and biaxial loading damaged by transverse and longitudinal matrix cracks and crack-induced transverse and longitudinal delamination.

The authors have been asked to provide sufficient information in this paper to allow readers to reproduce the results if they wished. Consequently, the paper will repeat some important details of the analysis that have been already published in the literature (Zhang, Fan and Soutis, 1992; Kashtalyan and Soutis, 1999a,b; 2000a-c; 2001a,b; 2002a,b), Soutis and Kashtalyan (2002) and Kashtalyan and Soutis (2005, 2006, 2007).

2 EQUIVALENT CONSTRAINT MODEL

Figure 1 shows a schematic of the cross-ply $[0_m/90_n]_s$ laminate damaged by transverse and longitudinal delaminations growing from the tips of transverse cracks in the 90° plies and splits in the 0° plies. Transverse cracks and splits are assumed to be spaced uniformly and to span the full thickness and width of the 90° and 0° plies, while delaminations were assumed strip-shaped. Spacings between splits and transverse cracks are denoted respectively $2s_1$ and $2s_2$, and the length of longitudinal and transverse delaminations are denoted $2\ell_1$ and $2\ell_2$, respectively. A global set of Cartesian co-ordinates with the origin in the centre of the laminate is introduced, with x_1 -axis coinciding with the fibre direction in the 90° lamina and x_3 -axis directed through the laminate thickness. The laminate is subjected to general in-plane biaxial tension ($\bar{\sigma}_{11}$ and $\bar{\sigma}_{22}$) and shear loading ($\bar{\sigma}_{12}$).

In order to analyse in-situ constrain effect on the stiffness of a particular cracked lamina, Fan and Zhang (1993) introduced the Equivalent Constraint Model (ECM) of the damaged laminate. In the ECM laminate, all the laminae below and above the damaged lamina under consideration are replaced with homogeneous layers (I and II) having the equivalent constraining effect (Fig. 2). In-plane stiffness properties of the equivalent constraint layer can be obtained from the laminated plate theory once their stresses and strains are known from micromechanical analysis (Fan and Zhang, 1993). Theoretically, ECM does not impose any restrictions onto the laminate lay-up, and the approach was applied to analysis of cross-ply laminates by Kashtalyan and Soutis (1999a,b, 2000a,b) and quasi-isotropic laminate with matrix cracking in all but 0° layers by Zhang and Herrmann (1999).

Application of the ECM approach to cross-ply laminate damaged by transverse and longitudinal matrix cracks and transverse and longitudinal crack-induced delaminations is schematically shown in Fig. 3. Instead of considering the damaged laminate configuration shown on Fig. 1, the following two ECMs are analysed instead. In ECM1 (Fig. 3a), the 0° lamina (layer 1) contains damage explicitly, while 90° lamina (layer 2), damaged by transverse cracking and transverse delaminations, is replaced with the homogeneous layer with reduced stiffness. Likewise, in ECM2 (Fig. 3b), the 90° lamina (layer 2) is damaged explicitly, while the split 0° lamina is replaced with the homogeneous layer with reduced stiffness. All the quantities associated with the 0° lamina (layer 1) will be henceforth denoted by a sub- or superscript (1), whereas those associated with the 90° lamina (layer 2) with a sub- or superscript (2).

The reduced stiffness properties of the μ^{th} layer ($\mu = 1, 2$) damaged by transverse cracking and transverse delaminations (if $\mu = 2$) or splitting and longitudinal

delamination (if $\mu = 1$) can be calculated from the laminated plate theory, provided stresses and strains in the explicitly damaged μ^{th} layer are known from the analysis of the ECM μ (i.e. ECM1 if $\mu = 1$ and ECM2 if $\mu = 2$). The reduced elastic properties of the equivalently constraining layer κ , $\kappa \neq \mu$ required in the analysis of the ECM μ are supposed to be determined from the analysis of the ECM κ . Thus, the problems for ECM1 and ECM2 are inter-related, damage coupling effect is included in the residual stiffness analysis.

3 STRESS ANALYSIS

Due to the periodicity of damage configuration in the ECM μ , only their representative segments (Fig. 3), containing either a pair of splits or a single transverse crack as well as two strip-shaped delaminations, need to be considered. As the representative segments are symmetric with respect to the mid-plane and their material and geometry are noteworthy uniform in direction perpendicular to the $x_\mu 0x_3$ plane, the analysis can be further restricted to one quarter of the representative segments. The representative segments of ECM1 and ECM2 can be segregated into perfectly bonded ($\ell_\mu < |x_\mu| < s_\mu$) regions and locally delaminated ($|x_\mu| < \ell_\mu$, $\mu = 1,2$) regions, with no frictional contact between the layers in the latter.

In the perfectly bonded regions ($\ell_\mu < |x_\mu| < s_\mu$) of the ECM μ , stresses can be determined from the equilibrium equations (Kashtalyan and Soutis, 2000a)

$$\frac{d}{dx_\mu} \tilde{\sigma}_{j\mu}^{(\mu,k)} + (-1)^k \frac{\tau_j^{(\mu)}}{h_k} = 0, \quad \mu = 1,2 \quad j = 1,2 \quad k = 1,2 \quad (1)$$

Here $\tau_j^{(\mu)}$ are the peak shear stresses at the (0/90) interface of the ECM μ in the $x_\mu 0x_3$ plane; $\tilde{\sigma}_{pq}^{(\mu,k)}$, $p, q = 1, 2$ are the in-plane microstresses in the k^{th} layer of the ECM μ , i.e. the stresses averaged across the thickness of the k^{th} layer and the width of the ECM μ as indicated below (Kashtalyan and Soutis, 2000a)

$$\tilde{\sigma}_{pq}^{(\mu,k)} = \frac{1}{2w_\mu h_k} \int_{-h_k}^{h_k} \int_{-w_\mu}^{w_\mu} \sigma_{pq}^{(\mu,k)} dx_3 dx_k, \quad p, q = 1, 2 \quad (2)$$

In the locally delaminated region ($|x_\mu| \leq \ell_\mu$) of the ECM μ , the in-plane microstresses in the explicitly damaged μ^{th} layer vanish, i.e.

$$\tilde{\sigma}_{j\mu}^{(\mu,\mu)} = 0, \quad j, \mu = 1, 2 \quad (3)$$

The in-plane microstresses are related to the total stresses $\bar{\sigma}_{ij}$ applied to the laminate by the following equilibrium equations (Kashtalyan and Soutis, 2000a)

$$\chi \tilde{\sigma}_{ij}^{(\mu,1)} + \tilde{\sigma}_{ij}^{(\mu,2)} = (1 + \chi) \bar{\sigma}_{ij}, \quad i, j = 1, 2 \quad \chi = h_1 / h_2 \quad (4)$$

It is assumed that both the explicitly damaged and the equivalently constraining laminae in the ECM μ are homogeneous orthotropic, and their constitutive equations, in terms of the in-plane microstresses and microstrains, can be written as (Kashtalyan and Soutis, 2000a)

$$\begin{Bmatrix} \tilde{\sigma}_1^{(\mu,\mu)} \\ \tilde{\sigma}_2^{(\mu,\mu)} \\ \tilde{\sigma}_6^{(\mu,\mu)} \end{Bmatrix} = \begin{bmatrix} \hat{Q}_{11}^{(\mu)} & \hat{Q}_{12}^{(\mu)} & 0 \\ \hat{Q}_{12}^{(\mu)} & \hat{Q}_{22}^{(\mu)} & 0 \\ 0 & 0 & \hat{Q}_{66}^{(\mu)} \end{bmatrix} \begin{Bmatrix} \tilde{\epsilon}_1^{(\mu,\mu)} \\ \tilde{\epsilon}_2^{(\mu,\mu)} \\ \tilde{\epsilon}_6^{(\mu,\mu)} \end{Bmatrix} \quad (5a)$$

$$\begin{Bmatrix} \tilde{\sigma}_1^{(\mu,\kappa)} \\ \tilde{\sigma}_2^{(\mu,\kappa)} \\ \tilde{\sigma}_6^{(\mu,\kappa)} \end{Bmatrix} = \begin{bmatrix} Q_{11}^{(\kappa)} & Q_{12}^{(\kappa)} & 0 \\ Q_{12}^{(\kappa)} & Q_{22}^{(\kappa)} & 0 \\ 0 & 0 & Q_{66}^{(\kappa)} \end{bmatrix} \begin{Bmatrix} \tilde{\epsilon}_1^{(\mu,\kappa)} \\ \tilde{\epsilon}_2^{(\mu,\kappa)} \\ \tilde{\epsilon}_6^{(\mu,\kappa)} \end{Bmatrix} \quad \mu, \kappa = 1, 2, \quad \kappa \neq \mu \quad (5b)$$

where $[\hat{Q}^{(\mu)}]$ denotes the in-plane stiffness matrix of the explicitly damaged μ^{th} layer (a circumflex (^) is used for representing the elastic properties of the undamaged material), and $[Q^{(\kappa)}]$, $\kappa \neq \mu$ denotes the in-plane stiffness matrix of the homogeneous orthotropic material of the equivalently constraining κ^{th} layer. The in-plane constitutive equations can also be written in terms of strains as (Kashtalyan and Soutis, 2000a)

$$\begin{Bmatrix} \tilde{\varepsilon}_1^{(\mu,\mu)} \\ \tilde{\varepsilon}_2^{(\mu,\mu)} \\ \tilde{\varepsilon}_6^{(\mu,\mu)} \end{Bmatrix} = \begin{bmatrix} \hat{S}_{11}^{(\mu)} & \hat{S}_{12}^{(\mu)} & 0 \\ \hat{S}_{12}^{(\mu)} & \hat{S}_{22}^{(\mu)} & 0 \\ 0 & 0 & \hat{S}_{66}^{(\mu)} \end{bmatrix} \begin{Bmatrix} \tilde{\sigma}_1^{(\mu,\mu)} \\ \tilde{\sigma}_2^{(\mu,\mu)} \\ \tilde{\sigma}_6^{(\mu,\mu)} \end{Bmatrix} \quad (6a)$$

$$\begin{Bmatrix} \tilde{\varepsilon}_1^{(\mu,\kappa)} \\ \tilde{\varepsilon}_2^{(\mu,\kappa)} \\ \tilde{\varepsilon}_6^{(\mu,\kappa)} \end{Bmatrix} = \begin{bmatrix} S_{11}^{(\kappa)} & S_{12}^{(\kappa)} & 0 \\ S_{12}^{(\kappa)} & S_{22}^{(\kappa)} & 0 \\ 0 & 0 & S_{66}^{(\kappa)} \end{bmatrix} \begin{Bmatrix} \tilde{\sigma}_1^{(\mu,\kappa)} \\ \tilde{\sigma}_2^{(\mu,\kappa)} \\ \tilde{\sigma}_6^{(\mu,\kappa)} \end{Bmatrix} \quad \kappa, \mu = 1,2 \quad \kappa \neq \mu \quad (6b)$$

where $[\hat{S}^{(\mu)}]$, $[S^{(\kappa)}]$, $\kappa \neq \mu$ denote the in-plane compliance matrices of the explicitly damaged μ^{th} layer and equivalently constraining κ^{th} layer, respectively.

In order to determine the in-plane microstresses in the perfectly bonded region from the equilibrium equations, Eq. (1), the interface shear stresses $\tau_j^{(\mu)}$ are expressed in terms of in-plane displacements $u_j^{(\mu,k)}$, $j = 1,2$. Here, it is assumed that the out-of-plane shear stresses $\sigma_{j3}^{(\mu,k)}$, $j = 1,2$ vary linearly with x_3 , which corresponds to a parabolic variation of the in-plane displacements. Besides that, it is assumed that in the 0° -lamina linear variation of the out-of-plane shear stresses $\sigma_{j3}^{(\mu,1)}$, $j = 1,2$, is restricted to the region of about one ply thickness (i.e. the nominal thickness of the pre-preg used to make the laminate). We assume that all layers of the laminate have thicknesses in the multiples of the nominal ply thickness. For laminates with thick 0° -layer this appears to offer a more reasonable description of the cracked laminate behaviour. For such laminates it was shown (Berthelot, 1997), by means of the finite element analysis, that

the assumption of parabolic variation of the in-plane displacements across the thickness of the whole 0°-layer provides a very poor approximation to the distribution of the longitudinal stress across the laminate thickness. This approximation becomes even poorer as the transverse crack density increases. Thus, here the out-of-plane shear stresses are assumed to vary as follows (Kashtalyan and Soutis, 2000a)

$$\begin{aligned} \sigma_{j3}^{(\mu,2)} &= \frac{\tau_j^{(\mu)}}{h_2} x_3 \quad |x_3| \leq h_2 & \sigma_{j3}^{(\mu,1)} &= \frac{\tau_j^{(\mu)}}{h_s} (h_2 + h_s - x_3) \quad h_2 \leq |x_3| \leq h_2 + h_s \\ \sigma_{j3}^{(\mu,1)} &= 0 \quad h_2 + h_s \leq |x_3| \leq h_2 + h_1 & h_s &= m_s t \quad j = 1,2 \end{aligned} \quad (7)$$

where h_s is the thickness of the shear layer, m_s is the number of plies in the shear layer, and t is the ply thickness. After some mathematical calculations and equation rearrangements (see Appendix A), the interface shear stresses are obtained as (Kashtalyan and Soutis, 2000a)

$$\tau_j^{(\mu)} = K_j^{(\mu)} (\tilde{u}_j^{(\mu,1)} - \tilde{u}_j^{(\mu,2)}) \quad (8)$$

where the shear lag parameters K_j are functions of ply properties (Kashtalyan and Soutis, 2000a)

$$K_j = \frac{3\hat{G}_{j3}^{(1)}\hat{G}_{j3}^{(2)}}{h_2\hat{G}_{j3}^{(1)} + (1 + (1 - \eta) / 2)\eta h_1\hat{G}_{j3}^{(2)}}, \quad \eta = h_s / h_1, \quad j = 1,2 \quad (9)$$

Here, $\hat{G}_{j3}^{(k)}$, $k = 1,2$ are the out-of-plane shear moduli of the k^{th} layer. As the presence of aligned microcracks does not affect the value of the out-of-plane shear moduli (this fact is emphasised by marking them with a circumflex (^)), the shear lag parameters K_j are the same for ECM1 and ECM2.

The equilibrium equations, Eq. (1), along with expressions for the interface shear stresses, Eq. (8), the laminate equilibrium equations, Eq. (4), and constitutive equations, Eq. (6), provide a full set of equations, which are required for determining the in-plane

microstresses $\tilde{\sigma}_{j\mu}^{(\mu,\mu)}$ $j, \mu = 1, 2$ in the perfectly bonded regions of the representative segment of the ECM μ . For instance, $\tilde{\sigma}_{11}^{(1,1)}$ can be found from the following set of 8 equations with respect to 8 variables (Kashtalyan and Soutis, 2000a)

$$\frac{d\tilde{\sigma}_{11}^{(1,1)}}{dx_1} - \frac{\tau_1^{(1)}}{h_1} = 0, \quad \tau_1^{(1)} = K_1(\tilde{u}_1^{(1,1)} - \tilde{u}_1^{(1,2)}) \quad (10a,b)$$

$$\chi\tilde{\sigma}_{11}^{(1,1)} + \tilde{\sigma}_{11}^{(1,2)} = (1 + \chi)\bar{\sigma}_{11}, \quad \chi\tilde{\sigma}_{22}^{(1,1)} + \tilde{\sigma}_{22}^{(1,2)} = (1 + \chi)\bar{\sigma}_{22} \quad (10c,d)$$

$$\left\{ \begin{array}{c} d\tilde{u}_1^{(1,1)} \\ dx_1 \\ \bar{\varepsilon}_2^{(1)} \end{array} \right\} = \begin{bmatrix} \hat{S}_{11}^{(1)} & \hat{S}_{12}^{(1)} \\ \hat{S}_{12}^{(1)} & \hat{S}_{22}^{(1)} \end{bmatrix} \left\{ \begin{array}{c} \tilde{\sigma}_{11}^{(1,1)} \\ \tilde{\sigma}_{22}^{(1,1)} \end{array} \right\}, \quad \left\{ \begin{array}{c} d\tilde{u}_1^{(1,2)} \\ dx_1 \\ \bar{\varepsilon}_2^{(1)} \end{array} \right\} = \begin{bmatrix} S_{11}^{(2)} & S_{12}^{(2)} \\ S_{12}^{(2)} & S_{22}^{(2)} \end{bmatrix} \left\{ \begin{array}{c} \tilde{\sigma}_{11}^{(1,2)} \\ \tilde{\sigma}_{22}^{(1,2)} \end{array} \right\} \quad (10e,f)$$

After some rearrangement, this and other similar sets of equations can be reduced to the single differential equations (Kashtalyan and Soutis, 2000a)

$$\frac{d^2 \tilde{\sigma}_{\mu\mu}^{(\mu,\mu)}}{dx_\mu} - L_1^{(\mu)} \tilde{\sigma}_\mu^{(\mu,\mu)} + \Omega_{11}^{(\mu)} \bar{\sigma}_{11} + \Omega_{22}^{(\mu)} \bar{\sigma}_{22} = 0, \quad \mu = 1, 2 \quad (11a)$$

$$\frac{d^2 \tilde{\sigma}_{12}^{(\mu,\mu)}}{dx_\mu} - L_2^{(\mu)} \tilde{\sigma}_{12}^{(\mu,\mu)} + \Omega_{12}^{(\mu)} \bar{\sigma}_{12} = 0 \quad (11b)$$

where $L_1^{(\mu)}, L_2^{(\mu)}, \Omega_{11}^{(\mu)}, \Omega_{22}^{(\mu)}, \Omega_{12}^{(\mu)}$ are the laminate constants depending on the layer compliances $\hat{S}_{ij}^{(\mu)}, S_{ij}^{(\kappa)}, \kappa \neq \mu$, shear lag parameters K_j and the layer thickness ratio $\chi = h_1 / h_2$. In detail, they are presented in Appendix B. Given the stress-free boundary conditions at the crack/split surfaces, solutions to Eqs. (11) are (Kashtalyan and Soutis, 2000a)

$$\tilde{\sigma}_{\mu\mu}^{(\mu,\mu)} = \frac{1}{L_1^{(\mu)}} \left(1 - \frac{\cosh[\sqrt{L_1^{(\mu)}}(x_\mu - s_\mu)]}{\cosh[\sqrt{L_1^{(\mu)}}(s_\mu - \ell_\mu)]} \right) (\Omega_{11}^{(\mu)} \bar{\sigma}_{11} + \Omega_{22}^{(\mu)} \bar{\sigma}_{22}) \quad (12a)$$

$$\tilde{\sigma}_{12}^{(\mu,\mu)} = \frac{1}{L_2^{(\mu)}} \left(1 - \frac{\cosh[\sqrt{L_2^{(\mu)}}(x_\mu - s_\mu)]}{\cosh[\sqrt{L_2^{(\mu)}}(s_\mu - \ell_\mu)]} \right) \Omega_{12}^{(\mu)} \bar{\sigma}_{12} \quad (12b)$$

where s_μ is crack/split half-spacing and ℓ_μ is crack/split tip delamination half-length (Figs. 1, 3). Once the in-plane microstresses, Eq. (12), in the explicitly damaged μ^{th} layer of the ECM μ are known, the laminate macrostresses can be found as (Kashtalyan and Soutis, 2000a)

$$\bar{\sigma}_{j\mu}^{(\mu,\mu)} = \frac{1}{2s_\mu} \int_{-s_\mu}^{s_\mu} \tilde{\sigma}_{j\mu}^{(\mu,\mu)} dx_\mu \quad (13)$$

The reduced stiffness properties of the layer μ , damaged by transverse cracking or splitting and delaminations, can be determined by applying the laminate plate theory to the ECM μ after replacing the explicitly damaged layer with an equivalent homogeneous one. The constitutive equations for the homogeneous layer equivalent to the explicitly damaged μ^{th} layer are (Kashtalyan and Soutis, 2000a)

$$\{\bar{\sigma}^{(\mu,\mu)}\} = [Q^{(\mu)}] \{\bar{\varepsilon}^{(\mu,\mu)}\} \quad (14)$$

Where in order to satisfy compatibility the macrostrains are assumed to be (Kashtalyan and Soutis, 2000a)

$$\bar{\varepsilon}_j^{(\mu,\mu)} = \bar{\varepsilon}_j^{(\mu,\kappa)} = \bar{\varepsilon}_j = \frac{1}{2s_\mu} \int_{-s_\mu}^{s_\mu} \tilde{\varepsilon}_j^{(\mu,\kappa)} dx_\mu, \quad \kappa \neq \mu, \quad j = 1,2,6 \quad (15)$$

4 STIFFNESS OF A DAMAGED LAMINA

The in-plane reduced stiffness matrix $[Q^{(\mu)}]$ of the homogeneous layer equivalent to the μ^{th} layer of the ECM μ is (Kashtalyan and Soutis, 2000a)

$$[Q^{(\mu)}] = [\hat{Q}^{(\mu)}] - [R^{(\mu)}] \quad (16)$$

$$[R^{(1)}] = \begin{bmatrix} \hat{Q}_{11}^{(1)} \Lambda_{22}^{(1)} & \hat{Q}_{12}^{(1)} \Lambda_{22}^{(1)} & 0 \\ \hat{Q}_{12}^{(1)} \Lambda_{22}^{(1)} & \frac{(\hat{Q}_{12}^{(1)})^2}{\hat{Q}_{11}^{(1)}} \Lambda_{22}^{(1)} & 0 \\ 0 & 0 & \hat{Q}_{66}^{(1)} \Lambda_{66}^{(1)} \end{bmatrix} \quad (17a)$$

$$[R^{(2)}] = \begin{bmatrix} \frac{(\hat{Q}_{12}^{(1)})^2}{\hat{Q}_{22}^{(2)}} \Lambda_{22}^{(1)} & \hat{Q}_{12}^{(1)} \Lambda_{22}^{(1)} & 0 \\ \hat{Q}_{12}^{(1)} \Lambda_{22}^{(1)} & \hat{Q}_{22}^{(1)} \Lambda_{22}^{(1)} & 0 \\ 0 & 0 & \hat{Q}_{66}^{(1)} \Lambda_{66}^{(1)} \end{bmatrix} \quad (17b)$$

The In-situ Damage Effective Functions $\Lambda_{22}^{(\mu)}$, $\Lambda_{66}^{(\mu)}$ introduced in (Fan and Zhang, 1993) can be expressed in terms of macrostresses and macrostrains in the μ^{th} layer of the ECM μ as (Kashtalyan and Soutis, 2000a)

$$\Lambda_{22}^{(1)} = 1 - \frac{\bar{\sigma}_{11}^{(1,1)}}{\hat{Q}_{11}^{(1)} \bar{\varepsilon}_1^{(1,1)} + \hat{Q}_{12}^{(1)} \bar{\varepsilon}_2^{(1,1)}} \quad (18a)$$

$$\Lambda_{22}^{(2)} = 1 - \frac{\bar{\sigma}_{22}^{(2,2)}}{\hat{Q}_{12}^{(2)} \bar{\varepsilon}_1^{(2,2)} + \hat{Q}_{22}^{(2)} \bar{\varepsilon}_2^{(2,2)}} \quad (18b)$$

$$\Lambda_{66}^{(\mu)} = 1 - \frac{\bar{\sigma}_{12}^{(\mu,\mu)}}{\hat{Q}_{66}^{(\mu)} \bar{\varepsilon}_6^{(\mu,\mu)}} \quad (18c)$$

On substituting macrostresses, calculated from Eqs. (13), and macrostrains, calculated from Eq. (15), into Eq. (18), the closed form expressions for IDEFs are obtained. They represent $\Lambda_{22}^{(\mu)}$, $\Lambda_{66}^{(\mu)}$ as functions of relative cracking/splitting density $D_\mu^{mc} = h_\mu / s_\mu$, relative delamination area $D_\mu^{ld} = \ell_\mu / s_\mu$, the layer compliances $\hat{S}_{ij}^{(\mu)}$, $S_{ij}^{(\kappa)}$, $\kappa \neq \mu$, shear lag parameters K_j and the layer thickness ratio χ (Kashtalyan and Soutis, 2000a)

$$\Lambda_{qq}^{(\mu)} = \Lambda_{qq}^{(\mu)} (D_\mu^{mc}, D_\mu^{ld}, \hat{S}_{ij}^{(\mu)}, S_{ij}^{(\kappa)}, K_j, \chi) \quad (19)$$

In detail, the closed form expressions for the IDEFs for the μ^{th} layer of the ECM_μ are (Kashtalyan and Soutis, 2000a)

$$\Lambda_{22}^{(\mu)} = 1 - \frac{1 - \frac{D_\mu^{mc}}{\lambda_1^{(\mu)}(1 - D_\mu^{ld})} \tanh\left[\frac{\lambda_1^{(\mu)}(1 - D_\mu^{ld})}{D_\mu^{mc}}\right]}{\frac{1 + \lambda_1^{(\mu)} D_\mu^{ld}}{1 - D_\mu^{ld}} + \alpha_1^{(\mu)} \frac{D_\mu^{mc}}{\lambda_1^{(\mu)}(1 - D_\mu^{ld})} \tanh\left[\frac{\lambda_1^{(\mu)}(1 - D_\mu^{ld})}{D_\mu^{mc}}\right]}, \quad \mu = 1, 2, \quad (20a)$$

$$\Lambda_{66}^{(\mu)} = 1 - \frac{1 - \frac{D_\mu^{mc}}{\lambda_2^{(\mu)}(1 - D_\mu^{ld})} \tanh\left[\frac{\lambda_2^{(\mu)}(1 - D_\mu^{ld})}{D_\mu^{mc}}\right]}{\frac{1 + \lambda_2^{(\mu)} D_\mu^{ld}}{1 - D_\mu^{ld}} + \alpha_2^{(\mu)} \frac{D_\mu^{mc}}{\lambda_2^{(\mu)}(1 - D_\mu^{ld})} \tanh\left[\frac{\lambda_2^{(\mu)}(1 - D_\mu^{ld})}{D_\mu^{mc}}\right]}, \quad \mu = 1, 2, \quad (20b)$$

where the constants $\lambda_i^{(\mu)}, \alpha_i^{(\mu)}, i = 1, 2$ (Appendix C) depend solely on the layer compliances $\hat{S}_{ij}^{(\mu)}, S_{ij}^{(\kappa)}, \kappa \neq \mu$, shear lag parameters K_j and the layer thickness ratio χ .

The modified compliances $S_{ij}^{(\kappa)}, \kappa \neq \mu$ of the equivalently constraining' κ^{th} layer of the ECM_μ are determined from the analysis of the ECM_κ and therefore are functions of the IDEFs $\Lambda_{22}^{(\kappa)}, \Lambda_{66}^{(\kappa)}$. Thus, the IDEFs for the μ^{th} layer depend implicitly on the damage parameters $D_\kappa^{mc} = h_\kappa / s_\kappa, D_\kappa^{ld} = h_\kappa / \ell_\kappa$ associated with the κ^{th} layer.

The IDEFs for both layers form a system of simultaneous nonlinear algebraic equations (Kashtalyan and Soutis, 2000a)

$$\Lambda_{qq}^{(1)} = \Lambda_{qq}^{(1)}(D_1^{mc}, D_1^{ld}, \hat{S}_{ij}^{(1)}, S_{ij}^{(2)}(D_2^{mc}, D_2^{ld}, \hat{S}_{ij}^{(2)}, \Lambda_{qq}^{(2)}), \chi), \quad q = 2, 6 \quad (21a)$$

$$\Lambda_{qq}^{(2)} = \Lambda_{qq}^{(2)}(D_2^{mc}, D_2^{ld}, \hat{S}_{ij}^{(2)}, S_{ij}^{(1)}(D_1^{mc}, D_1^{ld}, \hat{S}_{ij}^{(1)}, \Lambda_{qq}^{(1)}), \chi), \quad q = 2, 6 \quad (21b)$$

This system is solved computationally in FORTRAN by a direct iterative procedure. It is carried out in such a way that the newly calculated IDEFs $\Lambda_{qq}^{(\mu)}$ are used to evaluate the reduced stiffnesses of the equivalently constraining κ^{th} layer repeatedly until the difference between two iterative steps meets the prescribed accuracy. Consequently, all

four IDEFs $\Lambda_{qq}^{(k)}$, $q = 2, 6$ $k = 1, 2$ are determined as functions of damage parameters $D_1^{mc}, D_2^{mc}, D_1^{ld}, D_2^{ld}$. If interactions between damage modes in different laminae are neglected, IDEFs associated with the μ^{th} layer will depend only on damaged parameters for that layer.

Verification of the ECM/2-D shear lag approach in absence of delaminations induced by transverse cracking and splitting was carried out in (Kashtalyan and Soutis, 1999b; 2000b; Katerelos et al, 2008). After comparison with other existing models (Hashin, 1987; Tsai and Daniel, 1992; Henaff-Gardin et al, 1996) describing stiffness reduction of CFRP and GFRP cross-ply laminates due to transverse cracking and splitting, the following conclusions were reached in (Kashtalyan and Soutis, 2000b). As far as the reduction of the Young's modulus is concerned, the new approach is in very good agreement with other models. Its predictions are closer to the lower bound established in (Hashin, 1987) than the results (Henaff-Gardin et al, 1996) based on the model (Henaff-Gardin et al, 1996). For the Poisson's ratio, the ECM/2-D shear lag approach predictions are close to those of (Henaff-Gardin et al, 1996), although for small values of the damage parameter (relative crack/split spacing) the reduction predicted by the ECM/2-D shear lag approach is greater than (Henaff-Gardin et al, 1996). Predictions based on the variational approach Hashin (1987) are far away from these results. The shear modulus reduction ratio predicted by Tsai and Daniel (1992) is, in the most of cases, within 10% of the ECM/2-D shear lag approach value. It is worth mentioning here that the model of Tsai and Daniel (1992) and the present ECM/2-D shear lag approach yield exactly the same analytical expression for the shear modulus reduction ratio due to transverse cracking, if the thickness of the shear layer in the ECM/2-D shear lag approach is taken equal to that of the 0° lamina, i.e. if $h_s = h_1$ (Kashtalyan and Soutis, 2000b):

$$\rho_G \equiv \frac{G_A}{\hat{G}_A} = \left[1 + \frac{1}{\chi} \frac{D_2^{mc}}{\lambda_2^{(2,2)}} \tanh \frac{\lambda_2^{(2,2)}}{D_2^{mc}} \right]^{-1} \quad (22)$$

For transverse cracking combined with splitting, Tsai and Daniel (1992) suggested a semi-empirical expression for the shear modulus reduction ratio based on the "superposition" of solutions for a single set of cracks as (Kashtalyan and Soutis, 2000b)

$$\rho_G = \left[1 + \chi \frac{D_1^{mc}}{\lambda_2^{(1,1)}} \tanh \frac{\lambda_2^{(1,1)}}{D_1^{mc}} + \frac{1}{\chi} \frac{D_2^{mc}}{\lambda_2^{(2,2)}} \tanh \frac{\lambda_2^{(2,2)}}{D_2^{mc}} \right]^{-1} \quad (23)$$

The value of the shear modulus reduction ratio obtained by Tsai and Daniel (1992) using the finite difference iteration appeared to be within 1% of the value given by Eq. (23). The present ECM/2-D shear lag model, if the interaction between transverse cracks and splits is neglected and the shear layer has the thickness of the 0° lamina, yields an expression (Kashtalyan and Soutis, 2000b)

$$\rho_G^* = \left[1 - \frac{D_1^{mc}}{\lambda_2^{(1,1)}} \frac{D_2^{mc}}{\lambda_2^{(2,2)}} \tanh \frac{\lambda_2^{(1,1)}}{D_1^{mc}} \tanh \frac{\lambda_2^{(2,2)}}{D_2^{mc}} \right] \times \left[1 + \chi \frac{D_1^{mc}}{\lambda_2^{(1,1)}} \tanh \frac{\lambda_2^{(1,1)}}{D_1^{mc}} + \frac{1}{\chi} \frac{D_2^{mc}}{\lambda_2^{(2,2)}} \tanh \frac{\lambda_2^{(2,2)}}{D_2^{mc}} + \frac{D_1^{mc}}{\lambda_2^{(1,1)}} \frac{D_2^{mc}}{\lambda_2^{(2,2)}} \tanh \frac{\lambda_2^{(1,1)}}{D_1^{mc}} \tanh \frac{\lambda_2^{(2,2)}}{D_2^{mc}} \right]^{-1} \quad (24)$$

It may be seen from Eqs. (23) and (24) that the two expressions differ by the underlined terms and $\rho_G^* \leq \rho_G$. In absence of splitting ($D_1^{mc} = 0$) they are both reduced to Eq. (22). In some cases, though, the error of the semi-empirical expression, Eq. (23) suggested by Tsai and Daniel (1992) can be as big as 20%. The ECM/2-D shear lag approach is in good agreement with the results presented in (Henaff-Gardin et al, 1996) for the shear modulus reduction.

5 RESULTS AND DISCUSSION

In this section, the ECM/2-D shear lag approach is applied to predicting degraded stiffness properties of $[0/90/0]$ and $[0/90_g/0]$ cross-ply laminates under biaxial loading damaged by transverse and longitudinal matrix cracks. The laminates correspond to those of Test Cases (3) and (4) provided by the organisers of the exercise. Kaddour et al (2012c). Stiffness properties of a glass/LY556 material system used in the calculations are as follows: longitudinal modulus $E_1=45.6$ GPa, transverse modulus $E_2=16.2$ GPa, in-plane shear modulus $G_{12}=5.83$ GPa, through-thickness shear modulus $G_{23}=5.7$ GPa, major Poisson's ratio $\nu_{12}=0.278$, though-thickness Poisson's ratio $\nu_{23}=0.4$, ply thickness 0.125 mm. The layers thicknesses h_1 and h_2 are determined from the laminate lay-up, thickness of the shear layer is taken as $h_s = t$.

Stiffness degradation in cross-ply laminate due to different damage modes and their combinations is examined below. All results given below were obtained taking into account the interaction between damage modes in the adjacent layers. Up to 12 iterations are required to solve a set of simultaneous non-linear equations, Eqs. (21) with accuracy of 10^{-9} . The number of iterations increases along with the crack density and relative delamination area.

Figure 4 shows stiffness degradation in $[0/90/0]$ and $[0/90_g/0]$ laminates as the function of the transverse crack density C_2 in the 90° layer. Longitudinal Young's modulus, shear modulus and major Poisson's ratio are normalised by their values in the undamaged state. As can be seen from Fig. 4a and 4b, all these properties undergo degradation as the matrix crack density increases, with Poisson's ratio appearing to be the most affected by transverse cracking. The thickness of the 90° layers play an important role, since the thicker the 90° layer, the bigger reduction is observed.

Transverse ply thickness and the thickness ratio of 90° layer to constraining 0° or ±θ layers are the important parameters controlling resistance to matrix cracking. Zhang, Fan and Soutis (1992b) proposed to use a resistance curve, analogous to the R-curve concept of classical fracture mechanics, as a measure of the composite resistance to crack initiation and growth

$$G(\sigma, D^{mc}) = G_R(D^{mc}), \quad G_R = G_{IC} + G_0(1 - \exp(-RD^{mc})) \quad (25)$$

where G is the strain energy release rate associated with matrix cracking, G_R is the laminate resistance to matrix cracking, G_{IC} is the critical energy release rate for damage nucleation, and G_0 and R are laminate constants. Parameters G_{IC} , G_0 and R are not independent of stacking sequence, but remain constant as long the thickness ratio of the constraining layer to 90° remains the same.

When a cross-ply laminate is subjected to biaxial loading matrix cracking may occur concurrently in both plies leading to formation of transverse and longitudinal matrix cracks. The combined effect of these cracks on stiffness properties of [0/90/0] laminate is shown in Fig. 5 for the case when the longitudinal and transverse crack densities are equal.

In cross-ply laminates with thick 90° layer subjected to uniaxial loading strip-shaped delaminations begin to initiate and grow from the tips of matrix cracks at the 0°/90° interface. The effect of these delaminations on stiffness properties of [0/90_g/0] laminate is shown in Fig. 6 as a function of relative delamination area. Transverse crack density is taken as 2 cracks/cm, and the values of normalised stiffness properties for $D_2 = 0$ correspond to stiffness degradation due to matrix cracking without delamination. It can be seen from Fig. 6 that crack-tip delamination contributes

significantly to stiffness degradation of the laminate, and therefore has to be taken into account in the post-initial failure models.

The results from the current method have been compared by Kaddour et al (2012d) with those obtained from other damage models. The comparison has shown that damage modelling is still an immature subject and further work is needed in order to incorporate the various damage modes into a single tool for a potential use by designers.

6 CONCLUSIONS

Although the approach described in this paper has not attempted to predict ultimate laminate failure, it does present a methodology for predicting degraded stiffness properties of the laminae and hence the laminate, in the case when there are various kinds of intra- and interlaminar damage interacting with each other are present in the same and/or adjacent plies of the laminate. The approach is based on the Equivalent Constraint Model (ECM) of the damaged laminate and takes into account damage mode interaction. Our predictions show that the effect of longitudinal matrix cracking is more pronounced on the Poisson's ratio than on the shear modulus; however the reduction in the shear modulus due to transverse delamination is the most significant when compared to the reduction observed in the axial or transverse elastic moduli.

Theoretically, ECM does not impose any restrictions onto the laminate lay-up, and the approach based on ECM was successfully applied to the prediction of degraded stiffness properties due to matrix cracking in all but 0° layers of quasi-isotropic laminates, similar to those used in Test Cases (6)-(8) of the present exercise (Zhang and Herrmann, 1999). It should be noted that for the model to be applied the type, location and amount

of damage present need to be specified. For this accurate and reliable structural health monitoring (SHM) techniques are urgently required, see Soutis and coworkers, 2000, 2005, 2010. Also the triggering of resin cracking and delamination could be delayed to higher applied loads if tougher resin systems are employed, Jumahat *et al.*, 2010.

ACKNOWLEDGMENTS

This research arises from work carried out under EPSRC/GR/L51348 grant. Financial support UK's Engineering and Physical Sciences Research Council is gratefully acknowledged.

APPENDICES

A. Assuming that $\frac{\partial u_3^{(\mu,k)}}{\partial x_1} = \frac{\partial u_3^{(\mu,k)}}{\partial x_2} = 0$, $k = 1,2$, the out-of-plane constitutive

equations are

$$\gamma_{j3}^{(\mu,k)} \approx \frac{\partial u_j^{(\mu,k)}}{\partial x_3} = \frac{1}{\hat{G}_{j3}^{(k)}} \sigma_{j3}^{(\mu,k)}, \quad k = 1,2 \quad (\text{A1})$$

where $\hat{G}_{j3}^{(k)}$ are the out-of-plane shear moduli of the k^{th} layer. As was already noted, these elastic constants are not undergoing reduction due to matrix cracking. For the inner layer, substitution of Eq. (7) into Eq. (A1) and repeated integration with respect to x_3 across the layer thickness yield

$$\tilde{u}_j^{(\mu,2)} - u_j^{(\mu,2)} \Big|_{x_3=h_2} = -\frac{\tau_j^{(\mu)} h_2}{3\hat{G}_{j3}^{(2)}} \quad (\text{A2})$$

For the outer layer, substitution of Eq. (7) into Eq. (A1) and integration with respect to x_3 across the thickness of the shear layer leads to

$$u_j^{(\mu,1)} - u_j^{(\mu,1)} \Big|_{x_3=h_2} = -\frac{\tau_j^{(\mu)}}{h_s \hat{G}_{j3}^{(2)}} [(h_2 + h_s)(x_3 - h_2) - (x_3^2 - h_2^2)/2], \quad (\text{A3})$$

$$h_2 \leq x_3 \leq h_2 + h_s$$

On integrating Eq. (A3) across the thickness of the shear layer again, we obtain

$$\tilde{u}_j^{(\mu,1)} - u_j^{(\mu,1)} \Big|_{x_3=h_2} = \frac{\tau_j^{(\mu)} h_s}{3\hat{G}_{j3}^{(1)}}, \quad \mu, j = 1,2 \quad (\text{A4})$$

where $\tilde{u}_j^{(\mu,1)}$ are the displacements averaged across the thickness of the shear layer. In the part of the outer layer $h_2 + h_s \leq x_3 \leq h_2 + h_1$, free from the out-of-plane shear, the displacements $\tilde{\tilde{u}}_j^{(\mu,1)}$ are constant across the thickness and can be found from Eq. (A3) by putting $x_3 = h_2 + h_s$ as

$$\tilde{u}_j^{(\mu,1)} - u_j^{(\mu,1)} \Big|_{x_3=h_3} = \frac{\tau_j^{(\mu)} h_s}{2\hat{G}_{j3}^{(1)}} \quad (\text{A5})$$

The displacements, averaged across the whole thickness of the outer layer are then

$$\tilde{u}_j^{(\mu,1)} = \frac{1}{h_1} [h_s \tilde{u}_j^{(\mu,1)} + (h_1 - h_s) \tilde{u}_j^{(\mu,1)}] \quad (\text{A6})$$

Finally, the continuity of displacements at the interface due to the perfect bonding between the layers in the considered region should be taken into account, i.e.

$$u_j^{(\mu,1)} \Big|_{x_3=h_2} = u_j^{(\mu,1)} \Big|_{x_3=h_2} \quad (\text{A7})$$

Combining Eqs. (A2) and (A4–A7) yields Eq. (8) for the interface shear stresses $\tau_j^{(\mu)}$, with the shear lag parameters K_j given by Eq. (9).

$$\mathbf{B.} \quad L_1^{(1)} = \frac{K_1}{h_1} [\hat{S}_{11}^{(1)} + b_1 \hat{S}_{12}^{(1)} + \chi (S_{11}^{(2)} + b_1 S_{12}^{(2)})]$$

$$L_2^{(1)} = \frac{K_2}{h_1} [\hat{S}_{66}^{(1)} + \chi S_{66}^{(2)}]$$

$$\Omega_{11}^{(1)} = \frac{K_1}{h_1} (1 + \chi) (S_{11}^{(2)} + b_1 S_{12}^{(2)})$$

$$\Omega_{22}^{(1)} = \frac{K_1}{h_1} (1 + \chi) (S_{12}^{(2)} + b_1 S_{22}^{(2)})$$

$$\Omega_{12}^{(1)} = \frac{K_2}{h_1} (1 + \chi) S_{66}^{(2)}$$

$$L_1^{(2)} = \frac{K_2}{h_1} [S_{22}^{(1)} + a_1 S_{12}^{(1)} + \chi (\hat{S}_{22}^{(2)} + a_1 \hat{S}_{12}^{(2)})]$$

$$L_2^{(2)} = \frac{K_1}{h_1} [S_{66}^{(1)} + \chi \hat{S}_{66}^{(2)}]$$

$$\Omega_{11}^{(2)} = \frac{K_2}{h_1} (1 + \chi)(S_{12}^{(1)} + a_1 S_{11}^{(1)})$$

$$\Omega_{22}^{(2)} = \frac{K_2}{h_1} (1 + \chi)(S_{22}^{(1)} + a_1 S_{12}^{(1)})$$

$$\Omega_{12}^{(1)} = \frac{K_1}{h_1} (1 + \chi) S_{66}^{(1)}$$

$$a_1 = -\frac{S_{12}^{(1)} + \chi \hat{S}_{12}^{(2)}}{S_{11}^{(1)} + \chi \hat{S}_{11}^{(2)}} \quad b_1 = -\frac{\hat{S}_{12}^{(1)} + \chi S_{12}^{(2)}}{\hat{S}_{22}^{(1)} + \chi S_{22}^{(2)}} \quad \chi = \frac{h_1}{h_2}$$

K_1, K_2 are the shear lag parameters, Eq. (12).

$$\mathbf{C.} \quad \lambda_1^{(k)} = h_k \sqrt{L_1^{(k)}}, \quad k=1,2 \quad \lambda_2^{(k)} = h_k \sqrt{L_2^{(k)}}, \quad k=1,2$$

$$\alpha_1^{(1)} = \chi [\hat{Q}_{11}^{(1)} (S_{11}^{(2)} + b_1 S_{12}^{(2)}) + \hat{Q}_{12}^{(1)} (S_{12}^{(2)} + b_1 S_{22}^{(2)})]$$

$$\alpha_2^{(1)} = \chi \hat{Q}_{66}^{(1)} S_{66}^{(2)}$$

$$\alpha_1^{(2)} = \frac{1}{\chi} [\hat{Q}_{22}^{(2)} (S_{22}^{(1)} + a_1 S_{12}^{(1)}) + \hat{Q}_{12}^{(2)} (S_{12}^{(1)} + a_1 S_{11}^{(1)})]$$

$$\alpha_2^{(2)} = \frac{1}{\chi} \hat{Q}_{66}^{(2)} S_{66}^{(1)}$$

REFERENCES

Berthelot J.M. Analysis of the transverse cracking of cross-ply laminates: a generalised approach. *Journal of Composite Materials* 1997; 31(18), 1780-1805.

Bogetti T.A, Hoppel C.P.R., Harik V.M., Newill J.F., Burns B.P. Predicting the nonlinear response and progressive failure of composite laminates. *Composites Science and Technology* 2004; 64 (3-4), 329-342.

Bogetti T.A., Hoppel C.P.R., Harik V.M., Newill J.F., Burns B.P. Predicting the nonlinear response and progressive failure of composite laminates: correlation with experimental results. *Composites Science and Technology* 2004; 64 (3-4), 477-485.

Cuntze R.G. The predictive capability of failure mode concept-based strength criteria for multi-directional laminates—part B. *Composites Science and Technology* 2004; 64 (3-4), 487-516.

Cuntze R.G., Freund A. The predictive capability of failure mode concept-based strength criteria for multidirectional laminates. *Composites Science and Technology* 2004; 64 (3-4), 343-377.

Diamanti, K. and Soutis, C. “Structural health monitoring techniques for aircraft composite structures”. *Progress in Aerospace Sciences*, 46(8), (2010), 343-352.

Diamanti, K., Soutis, C. and Hodgkinson, J. M. “Lamb waves for the non-destructive inspection of monolithic and sandwich composite beams”. *Composites A*, 36(2), (2005), 189-195.

Diaz Valdes, S.H. and Soutis, C. “Health monitoring of composites using Lamb waves generated by piezo-electric devices”. *Plastics, Rubber and Composites*, 29(9), (2000), 496-502.

Fan J., Zhang J. In-situ damage evolution and micro/macro transition for laminated composites. *Composites Science and Technology* 1993; 47: 107-118.

Hashin Z. Analysis of orthogonally cracked laminate under tension. *Transactions of ASME Journal of Applied Mechanics* 1987; 54, 872-879.

Henaff-Gardin C., Lafarie-Frenot M.C., Gamby D. Doubly periodic matrix cracking in composite laminates Part 1: General in-plane loading. *Composite Structures* 1996; 36(1-2), 113-130.

Henaff-Gardin C., Lafarie-Frenot M.C., Gamby D. Doubly periodic matrix cracking in composite laminates Part 2: Thermal biaxial loading. *Composite Structures* 1996; 36(1-2), 131-140.

Jumahat, A., Soutis, C., Jones, F.R. and Hodzic, A. Fracture mechanisms and failure analysis of carbon fibre/toughened epoxy composites subjected to compressive loading. *Composite Structures*, 92(2), (2010), 295-305.

Kaddour A.S., Hinton M.J., Soden P.D. A comparison of the predictive capabilities of current failure theories for composite laminates: additional contributions. *Composites Science and Technology* 2004; 64 (3-4), 2004, 449-476.

Kaddour A S and Hinton M J. Maturity of 3D failure criteria for fibre reinforced composites: Comparison between theories and experiments: Part B of WWFE-II. To be published in *J Compos Mater* (2012a).

Kaddour A S, Hinton M J, Li S and Smith P A. The Background To Part A of The Third World-Wide Failure Exercise (WWFE-III). To be published in *J Compos Mater* (2012b).

Kaddour, A.S., M. J. Hinton, S Li and P.A. Smith, Mechanical properties and details of composite laminates for the test cases used in the third world wide failure exercise. To be published in J Compos Mater (2012c).

Kaddour A S, Hinton M J, Smith P A and Li S. A comparison between the predictive capability of current matrix cracking, continuum damage and fracture criteria for fibre reinforced composite laminates: Part A of WWFE-III. To be published in J Compos Mater (2012d).

Kashtalyan M., Soutis C. Stiffness and fracture analysis of laminated composites with off-axis ply matrix cracking. Composites Part A: Applied Science and Manufacturing 2007; 38(4), 1262-1269.

Kashtalyan M., Soutis C. Modelling off-axis ply matrix cracking in continuous fibre-reinforced polymer matrix composite laminates. Journal of Materials Science 2006; 41(20), 6789-6799.

Kashtalyan M., Soutis C. Analysis of composite laminates with intra- and interlaminar damage. Progress in Aerospace Sciences 2005; 41(2), 152-173.

Kashtalyan M., Soutis C. Mechanisms of internal damage and their effect on the behavior and properties of cross-ply composite laminates. International Applied Mechanics 2002; 38(6), 641-657.

Kashtalyan M., Soutis C. Analysis of local delaminations in composite laminates with angle ply matrix cracks. International Journal of Solids and Structures 2002; 39(6), 1515-1537.

Kashtalyan M., Soutis C. Strain energy release rate for off-axis ply cracking in laminated composites. International Journal of Fracture 2001; 112 (2), L3-L8.

Kashtalyan M., Soutis C. Stress analysis of angle-ply laminates with matrix cracks. ZAMM 2001; 81, Supplement 2, S371-S372.

Kashtalyan M., Soutis C. Modelling stiffness degradation due to matrix cracking in angle-ply composite laminates. *Plastics, Rubber and Composites* 2000; 29(9), 482-488.

Kashtalyan M., Soutis C. Stiffness degradation in cross-ply laminates damaged by transverse cracking and splitting. *Composites: Part A* 2000; 31(4), 335-351.

Kashtalyan M., Soutis C. The effect of delaminations induced by transverse cracking and splitting on stiffness properties of composite laminates. *Composites: Part A* 2000; 31(2), 107-119.

Kashtalyan M., Soutis C. Application of the Equivalent Constraint Model to investigate stiffness properties of transversally cracked and split FRP laminates. *Advanced Composites Letters* 1999; 8(5), 205-211.

Kashtalyan M., Soutis C. A study of matrix crack tip delaminations and their influence on composite laminate stiffness. *Advanced Composites Letters* 1999; 8(4), 149-156.

Katerelos D.T.G., Kashtalyan M., Soutis C., Galiotis C. Matrix cracking in polymeric composites laminates. Modelling and experiments. *Composites Science and Technology* 2008; 68(12), 2310-2317.

Kuraishi A., Tsai S.W., Liu K.S. A progressive quadratic failure criterion, part B. *Composites Science and Technology* 2002; 62 (12-13), 1683-1695.

Liu K.S., Tsai S.W. A progressive quadratic failure criterion for a laminate. *Composites Science and Technology* 1998; 58(7), 1023-1032.

McCartney L.N. Predicting transverse crack formation in cross-ply laminates *Composites Science and Technology* 1998; 58 (7), 1069-1081.

McCartney L.N. Prediction of ply crack formation and failure in laminates

Composites Science and Technology 2002; 62(12-13), 1619-1631

Puck A., Schürmann A. Failure analysis of FRP laminates by means of physically based phenomenological models. Composites Science and Technology 1998; 58 (7), 1045-1067.

Puck A., Schürmann A. Failure analysis of FRP laminates by means of physically based phenomenological models. Composites Science and Technology 2002; 62 (12-13), 1633-1662.

Soden P.D., Kaddour A.S., Hinton M.J. Recommendations for designers and researchers resulting from the world-wide failure exercise. Composites Science and Technology 2004; 64 (3-4), 589-604.

Soutis C., Kashtalyan M. Delamination growth and residual properties of cracked orthotropic laminates under tensile loading. Journal of Thermoplastic Composite Materials 2002; 15(1), 13-22.

Tsai C.L., Daniel I.M. Behavior of cracked cross-ply composite laminate under shear loading. International Journal of Solids and Structures 1992; 29(24), 3251-3267.

Zinoviev P.A., Grigoriev S.V., Lebedeva O.V., Tairova L.R. The strength of multilayered composites under a plane-stress state. Composites Science and Technology 1998; 58 (7), 1209-1223.

Zinoviev P.A., Grigoriev S.V., Lebedeva O.V., Tairova L.R. A coupled analysis of experimental and theoretical results on the deformation and failure of composite laminates under a state of plane stress. Composites Science and Technology 2002; 62 (12-13), 1711-1723.

Zhang D., Ye J., Lam D. Ply cracking and stiffness degradation in cross-ply laminates under biaxial extension, bending and thermal loading. *Composite Structures* 2006; 75(1-4); 121-131.

Zhang J., Fan J., Soutis C. Analysis of multiple matrix cracking in composite laminates. Part 1: In-plane stiffness properties. *Composites* 1992; 23(9); 291-298.

Zhang J., Fan J., Soutis C. Analysis of multiple matrix cracking in composite laminates. Part 2: Development of transverse ply cracks. *Composites* 1992; 23(9); 299-294.

Zhang J., Herrmann K.P. Stiffness degradation induced by multilayer intralaminar cracking in composite laminates. *Composites Part A: Applied Science and Manufacturing* 1999; 30(5), 683-706.

FIGURE CAPTIONS

FIGURE 1. Cross-ply laminate damaged by transverse and longitudinal matrix cracks and transverse and longitudinal crack-induced delaminations.

FIGURE 2. Equivalent Constraint Model (ECM) of a damaged laminate: a) initial laminate; b) ECM k .

FIGURE 3. Representative segments of the two equivalent constraint models: a) ECM1; b) ECM2.

FIGURE 4. Normalised stiffness properties of glass/epoxy cross-ply laminates as a function of transverse crack density in the 90° layer: a) [0/90/0] laminate; b) [0/90₈/0] laminate. No damage in the 0° layer (uniaxial tensile loading, static or fatigue).

FIGURE 5. Normalised stiffness properties of glass/epoxy [0/90/0] cross-ply laminate as a function of transverse crack density in the 90° layer, equal to longitudinal crack density (equi-biaxial tensile static or fatigue loading).

FIGURE 6. Normalised stiffness properties of glass/epoxy [0/90₈/0] cross-ply laminate as a function of transverse delamination area. Transverse crack density 2 cracks/cm (uniaxial tensile loading).

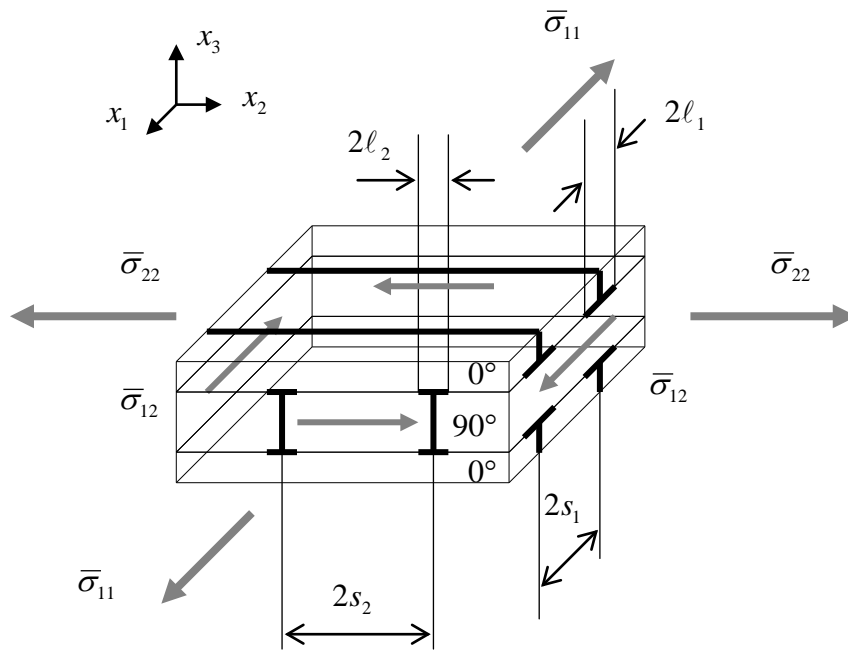


Figure 1

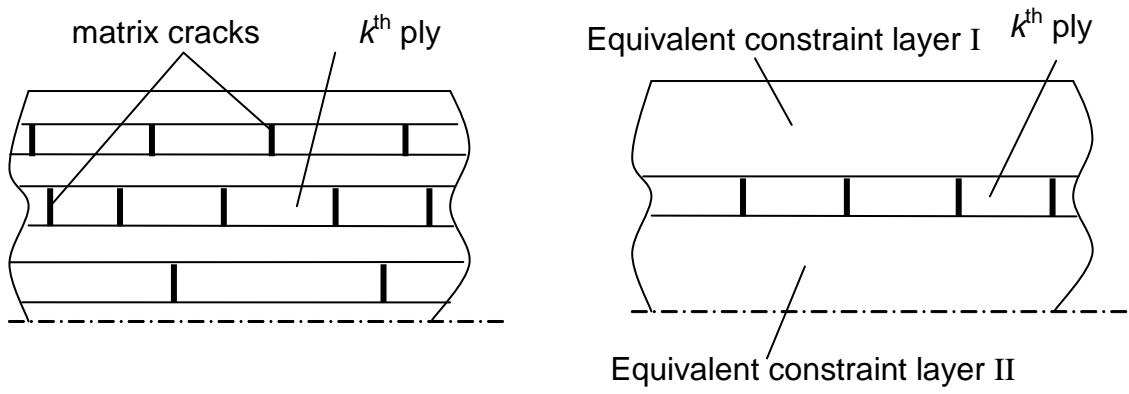


Figure 2

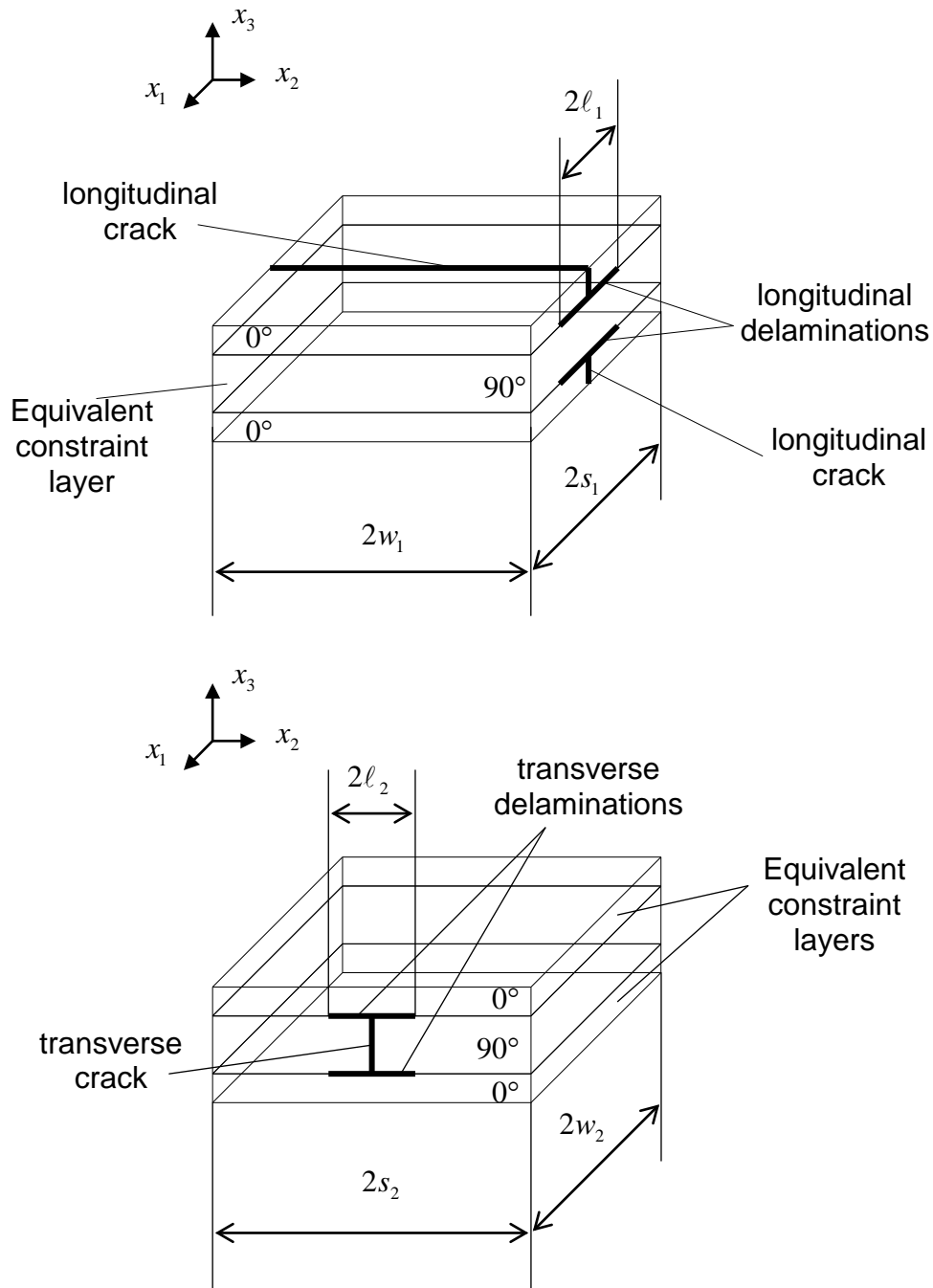
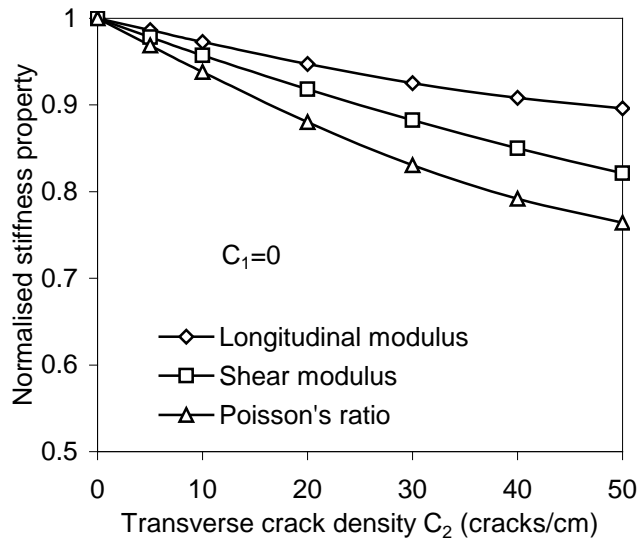
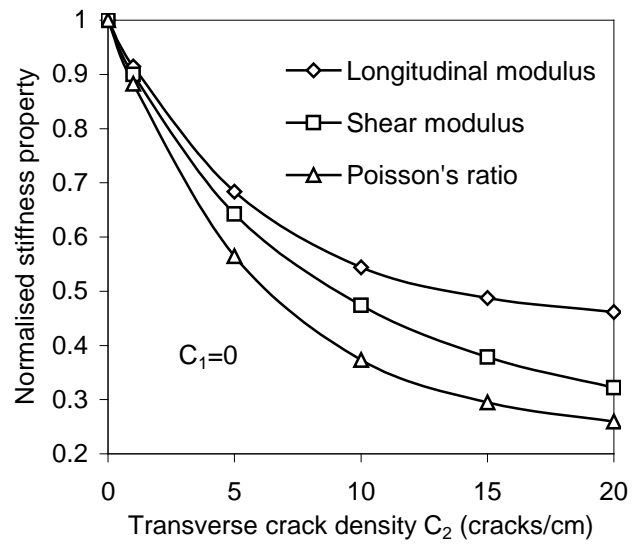


Figure 3



a)



b)

Figure 4

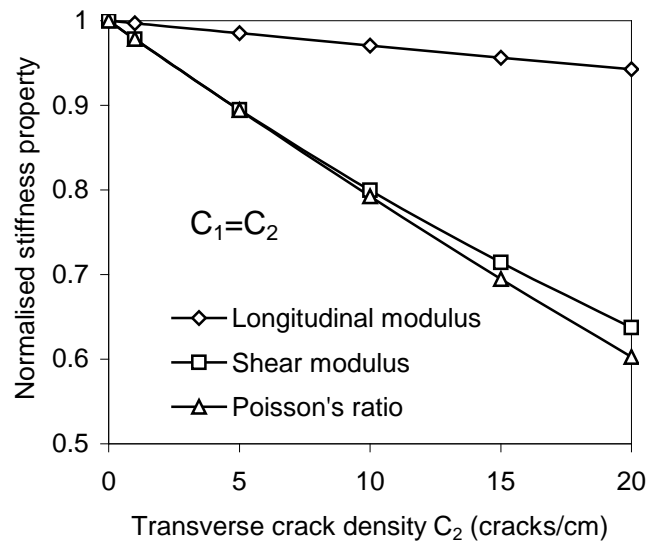


Figure 5

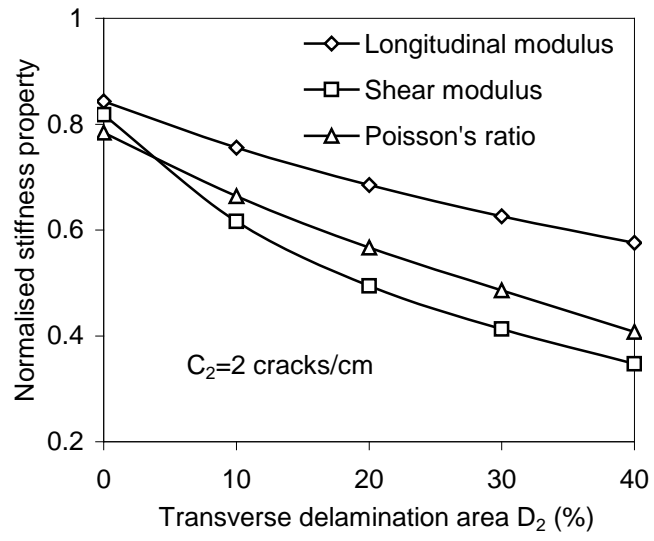


Figure 6